Artifact-free reconstruction from off-axis digital holograms through nonlinear filtering

Nicolas Pavillon[1], Chandra Sekhar Seelamantula[2], Michael Unser[3], Christian Depeursinge[1]

[1]Advanced Photonics Laboratory (MVD), Ecole Polytechnique Fédérale de Lausanne (EPFL), CH-1015 Lausanne, Switzerland

[2]Department of Electrical Engineering, Indian Institute of Science, Bangalore, India

[3]Biomedical Imaging Group, Ecole Polytechnique Fédérale de Lausanne (EPFL), CH-1015 Lausanne, Switzerland

ABSTRACT

We present experimental investigation of a new reconstruction method for off-axis digital holographic microscopy (DHM). This method effectively suppresses the object auto-correlation, commonly called the zero-order term, from holographic measurements, thereby suppressing the artifacts generated by the intensities of the two beams employed for interference from complex wavefield reconstruction. The algorithm is based on non-linear filtering, and can be applied to standard DHM setups, with realistic recording conditions. We study the applicability of the technique under different experimental configurations, such as topographic images of microscopic specimens or speckle holograms.

Keywords: Digital holography, Image reconstruction technique, Interferometric imaging, Phase measurement.

1. INTRODUCTION

Digital holography (DH) is a measurement technique based on an interferometric principle, which enables the recovery of both the amplitude and phase of a wavefront. This method has been coupled with microscopy [1] for applications such as high-precision surface topography,[2] or biological investigations.[3–5] In the macroscopic case, this measurement method has been used in many different fields, such as quality check applications or vibration assessment. [6]

The principle of holography is based on the measurement of the interference between two waves, where one interacted with the specimen, commonly called the object wave, and a reference wave having a phase profile which is precisely controlled. The interference pattern is then measured in intensity on a photographic plate or an electronic system such as a charge-coupled device (CCD) camera. Due to this acquisition process, different terms are recorded: the intensities of both waves, usually referred to as the zero-order term, the object wavefront information, and, because of the real nature of the recorded signal, the complex conjugate of the object wave, called twin-image. This redundant information makes it more difficult to recover an accurate reconstruction of the object signal, and can even disrupt it.

Reconstructing the signal containing the information about the object complex wavefront requires separating it from the other terms contained in the interferogram. Two main methods have been employed to accomplish it, either in the spatial or temporal domain. Spatial separation has been performed by using a reference wave which propagation direction slightly differs from that of the object wave. In this off-axis configuration, the terms contained in the hologram propagate in different direction, making it possible to isolate the object wavefront. [7] More recently, this spatial separation has been performed digitally in the Fourier domain. [1] On the other hand, temporal separation can be achieved through the acquisition of several holograms, giving rise to phase-shifting interferometry (PSI) methods. [8] Phase-shifting is classically done with four-steps or three-steps algorithms.[9] However, these methods need very accurate and equally spaced phase-shifts, therefore requiring expensive devices. More recently, adaptive PSI has been

Further author information: (Send correspondence to Nicolas Pavillon)
N. Pavillon: E-mail: nicolas.pavillon@a3.epfl.ch

developed, making it possible to use holograms without accurately known phase-shifts, [10,11] at the cost of employing iterative procedures.

Different methods were proposed to suppress the zero-order term in off-axis holography. First, intensity terms were considered as constant, making it possible to subtract them with a constant term; [12] linear filtering was also used with high-pass filters.[13] Those methods have the drawback of altering the reconstructed signal, due to their global filtering effect. Non-linear methods were also proposed by employing approximations on the signal along with square operators,[14] or wavelet-based transforms by using a Taylor development. [15] Another method employing the logarithm operator has been proposed,[16] by neglecting the effect of the zero-order term in this context. The methods cited above always employ an approximation of the interference equation, or restrict the field of application by using strong assumptions on the type of object field.

The method presented in this paper is based on non-linear filtering, and provides exact reconstruction, if simple requirements are fulfilled. It can be applied to off-axis DHM, by filtering the hologram in the cepstral domain, which is defined as the logarithm of the Fourier transform of the signal. It has no restrictive requirements on the object nor on the reference. The two main conditions are that the reference amplitude must be stronger than that of the object, and that the desired imaging order has to be confined to one quadrant of the Fourier domain. Apart from those conditions which can be easily fulfilled in practice, the method is general. It is non-iterative and its computational cost is moderate. This technique suppresses the requirement of having a separation constraint between the zero-order and the diffraction terms, thereby extending the available spectral support of the image.

In previous publications,[17,18] we investigated this method to suppress the zero-order auto-correlation in digital holographic reconstruction. We showed that the proposed technique suppresses the zero-order term under realistic conditions. In this article, we address the robustness of the method for use with speckle holograms, and present experimental results demonstrating the suppression of the artifacts generated by the zero-order. We then extend our analysis on the improvement in spatial resolution.

2. FUNCTIONING PRINCIPLE

The method we propose is based essentially on the principles developed in spatial filtering method for digital holographic microscopy (DHM)[1,19,20] as classically implemented for off-axis holography. Our aim is to employ cepstral filtering in this context to improve the efficiency of zero-order filtering. We hereby recall the basic principles and necessary elements for characterizing the performance of the new technique.

2.1 Spatial filtering method

The interference pattern generated by the two beams used for measurement and recorded on the camera plane is

$$\begin{aligned} i(x,y) &= |r(x,y)+o(x,y)|^2 \\ &= |o(x,y)|^2 + |r(x,y)|^2 + o(x,y)^* r(x,y) + o(x,y) r(x,y)^*, \end{aligned} \tag{1}$$

where $o(x,y)$ is the object wave, $r(x,y)$ is the reference wave, and the asterisk denotes the complex-conjugate operator. The first two terms of Eq. (1) correspond to the so-called zero-order; the last two terms are the +1 and -1 diffraction orders, which are the real and virtual images, respectively. Using different propagation directions for the two interfering waves modulates the diffraction terms at a carrier spatial frequency, so that they do not overlap spectrally. This off-axis configuration leads to a Fourier plane corresponding to the one shown in Fig. 1(a). It thus makes it possible to recover one of the imaging order by Fourier filtering techniques (FT). [21] In this case, the object wavefront is given by

$$\begin{aligned} o^{FT}(x,y) &= r_D(x,y) i_F(x,y), \\ i_F(x,y) &= \mathscr{F}^{-1}\left\{\mathscr{F}\left\{i(x,y)\right\} \times W(\omega_x,\omega_y)\right\}, \end{aligned} \tag{2}$$

where $W(\omega_x,\omega_y)$ is the filtering window function in the frequency domain, and $i_F(x,y)$ is the filtered hologram; r_D is a digital reference wave, classically taken as the complex conjugate of the reference wave used during the experiment. In the case the hologram is acquired out-of-focus, such as in Fresnel digital holography, the complex wavefront can then be numerically propagated to the image plane by employing for instance the Fresnel approximation. [19,22]

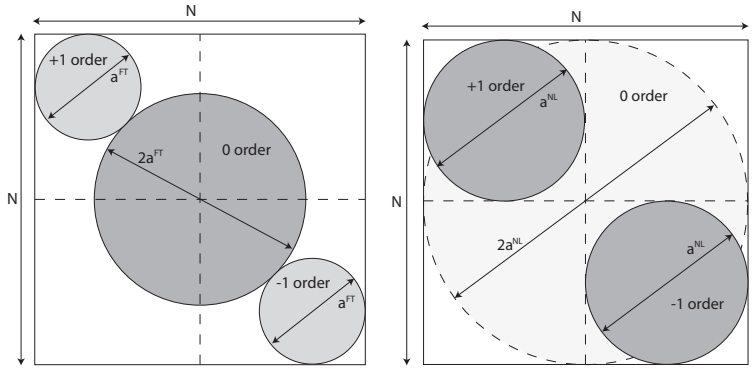

(a) (b)

Figure 1: Optimal spectral configuration of the Fourier transform of a hologram in the case of (a) standard Fourier technique (FT) and (b) non-linear (NL) reconstruction with object auto-correlation suppressed, improving the usable bandwidth for the imaging order.

2.2 Non-linear filtering

By rearranging the terms in Eq. (1) (spatial coordinates are omitted for the sake of brevity), we obtain

$$\frac{i}{|r|^2} = \left(1 + \frac{o}{r}\right)\left(1 + \left(\frac{o}{r}\right)^*\right). \tag{3}$$

Next, we can take the logarithm

$$\ln\left(\frac{i}{|r|^2}\right) = \ln\left(1 + \frac{o}{r}\right) + \ln\left(1 + \left(\frac{o}{r}\right)^*\right), \tag{4}$$

which transforms the product into a sum, allowing for the subsequent separation of the interference terms from the zero-order.

We have shown,[17] by employing the Taylor series expansion of the logarithm operator, that if the imaging order is confined in one quadrant of the Fourier spectrum, the terms on the right of Eq. (4) have their spectra contained in the same quadrant as the usual imaging orders o^*r and or^*. This development requires that the reference amplitude is higher than that of the object wave, i.e. $|r| > |o|$. As a result, the two terms can be filtered out spectrally.

It is therefore feasible to retain the desired imaging order by selecting the corresponding quadrant of the hologram spectrum. The signal is then recovered by the inverse Fourier transformation. In analogy with the classical filtering operation, the filtered diffraction order in the spatial domain can be calculated as

$$i'_F(x,y) = \ln\left(1 + \frac{o}{r}\right) = \mathscr{F}^{-1}\left\{\mathscr{F}\left\{\ln\left(\frac{i}{|r|^2}\right)\right\} \times \mathbf{1}_{[0,\infty)\times[0,\infty)}\right\}, \tag{5}$$

where the indicator function $\mathbf{1}_{[0,\infty)\times[0,\infty)}$ denotes the window used to select the relevant quadrant (in this particular case, the first quadrant). This filtering operation and the corresponding imaging terms are represented in Fig. 1(b). Finally, the recovered object wavefront in the hologram plane is given by

$$o^{NL}(x,y) = r_D(x,y)\left(\exp\left(i'_F(x,y)\right) - 1\right), \tag{6}$$

which specifies our non-linear filtering method (NL).

By comparing Eq. (2) and Eqs. (5-6), we find that the proposed algorithm is similar to the standard Fourier filtering method, except for the non-linear logarithm and exponential operations. The object complex wavefront is reconstructed by multiplying the filtered signal with a digital reference wave, as in standard off-axis DHM.

The technique described in this Section provides zero-order-free reconstruction, which makes it possible to extend the available spectral support for the imaging terms. The limit in the framework of this technique is the fact that the diffraction orders have to be contained in a quadrant of the Fourier plane. The optimal spectral configuration in this case is shown in Fig. 1(b), which provides an available bandwidth of $a^{NL} = N/2$, where N is the resolution of the recorded hologram in pixels. This corresponds to an enlargement of the bandwidth by a factor of approximately 1.5 times.[18]

2.3 Consequences of the non-linear method on experimental acquisition

The new technique just presented requires some specific conditions to be satisfied during hologram recording. The first condition, namely $|r| > |o|$, is usually readily fulfilled in a global sense, since it was shown that higher intensity in the reference wave yields a better signal-to-noise ratio (SNR) of the phase signal.[23] This condition may not be fulfilled for every pixel in the hologram plane, particularly in the case of out-of-focus images or speckle holograms, which may contain strong intensity regions, mainly induced by the highly-diffracting parts of the sample.

It is also required that the spectra of the +1 and -1 diffraction orders do not overlap. This condition is naturally fulfilled in the case of off-axis DHM. Confining the usable frequency space to one specific quadrant is equivalent to having interference fringes inclined at 45°, which corresponds to ideal measurement conditions, i.e. the best spatial sampling case for those high frequencies.

Moreover, as it can be seen from Eq. (5), prior knowledge of the reference intensity is required, since our algorithm suppresses the object zero-order, i.e. $|o|^2$, but not $|r|^2$. It corresponds in fact to a subtraction of $|r|^2$ before processing.

It should be noted that the reference is commonly assumed to be a plane wave, so that elimination of its intensity corresponds to simply subtracting a constant. However, some wavefront aberrations are always present in practice, which induce irregularities in the reconstructed signal. Nevertheless, our experimental results show that it is possible to counter those effects by simple subtraction of a reference intensity that is recorded during a calibration step, since the reference is classically a wave which profile is well controlled and constant during time.

3. SIMULATIONS

In this Section, we present simulation results based on the reconstruction of speckle holograms. In the case speckle is occurring, the object wave contains very high spatial frequencies, created by the random phase pattern generated by the specimen roughness. This can be identified in the spectrum of the generated hologram as an approximately constant spectral energy in the aperture of the optical system, as presented in Fig. 2(b).

The synthetic hologram is based on a representation of a USAF 1951 test target, containing specific spatial frequencies, as shown in Fig. 2(a). In order to simulate the roughness of the object, the phase has been set to a random value uniformly distributed between $[-\pi/2, \pi/2]$. This simulation considers a low aperture optical system, composed of a $2f$ lens system. The field diffracted by the specimen is propagated to the first lens of the optical system, where a low-pass filter is applied to account for the optical component aperture, and a curvature in phase is applied according to the focal length of the lens. The field is next propagated to the second lens where its curvature is compensated. Then, it is propagated to the hologram plane, where the interference with a tilted reference wave is computed. The reference wave has been designed so that its amplitude is slightly stronger than the maximum value of the object field, to satisfy the condition required by the non-linear reconstruction method. The optical system was taken for a numerical aperture of $\mathrm{NA} = 0.045$, a wavelength of $\lambda = 760$ nm and a pixel size of the camera of $\Delta x = 6.45$ μm. The amplitude of the object reconstructed through non-linear filtering is presented in Fig. 2(c), where the typical granular texture of speckle images can be readily identified. We compare in this case the standard reconstruction based on spatial filtering and the non-linear technique in the spectral domain. The Fourier transform of the hologram is presented in Fig. 2(b), where the zero-order can be identified in the center of the spectrum, clearly being twice the size of the imaging orders, situated in the two corners. The strong extent of the zero-order makes it impossible to filter clearly the imaging order without getting part of the auto-correlation in the reconstruction, which results in artifacts during reconstruction.

On the other hand, the spectrum of the object field after non-linear reconstruction is shown in Fig. 2(d), where zero-order has been suppressed. This can be readily seen by identifying the constant background around the imaging

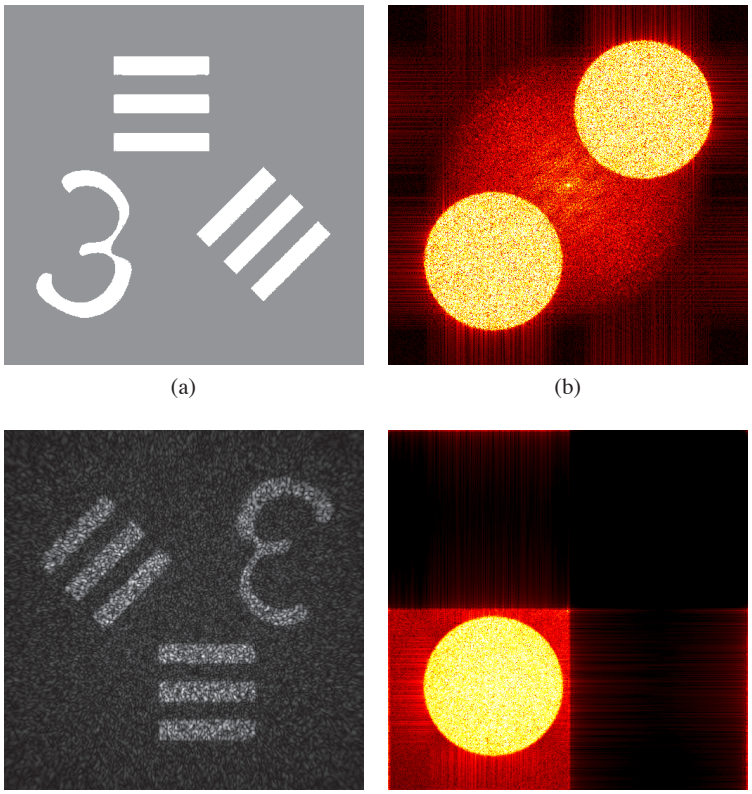

Figure 2: (a) Amplitude of the synthetic object used for simulation, and (b) Fourier transform of the speckle hologram generated from this object. (c) Amplitude of the object wavefront reconstructed with the non-linear method, after generation of the speckle hologram, corresponding to (d) a zero-order-free spectrum after reconstruction.

term, showing no zero-order left in the center of the spectrum. The three other quadrants were filtered out during the reconstruction process, as explained in Section 2.2 and shown in Eq. (5).

The simulation presented in this Section shows that non-linear reconstruction can be applied to rough samples, giving rise to speckle holograms. However, one should note that this type of signal can lead to several issues if not handled properly. The non-linear reconstruction method requires that the amplitude of the reference wave has to be strictly stronger than that of the object. This condition can be difficult to satisfy in the case of rough objects, in which case random constructive interferences can lead to strong intensities in the object wave.

4. EXPERIMENTS

The measurements presented in this Section were performed on a reflection digital holographic microscope [1] (cf. Fig. 3). The laser is split into two beams, with the first one reflecting on the specimen after having passed through the microscope objective (MO). The diffracted wave is collected by the MO, and interferes with the second beam, which curvature has been matched through a curvature lens. The resulting interference pattern is recorded in the Fresnel zone with a CCD camera. The reconstruction can then be performed according to the methods described in Section 2.

4.1 Speckle holograms

In order to demonstrate the applicability of our technique to speckle holograms, we measured the reflected field on a coin, which generates an approximately random phase, as it can identified in the spectrum of the hologram, shown in

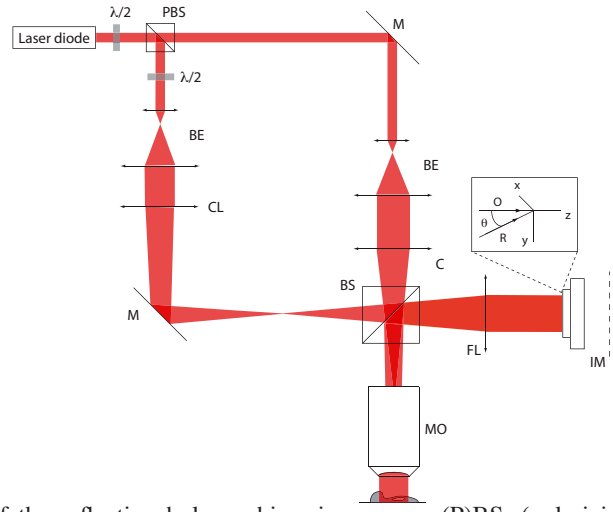

Figure 3: Optical sketch of the reflection holographic microscope. (P)BS: (polarizing) beamsplitter, $\lambda/2$: half-waveplate, M: mirror, BE: beam expander, C: condenser lens, MO: microscope objective, FL: field lens, IM: image plane, CL: curvature lens.

Fig. 4(a), where the constant spectral energy in the optical aperture indicates the random orientation of the reflected beam.

The coin was measured with a low aperture system, where the reflected field is collected with an achromatic lens, providing a magnification of $3\times$, with a laser wavelength of $\lambda = 760$ nm, in a configuration similar to the one shown in Fig. 3.

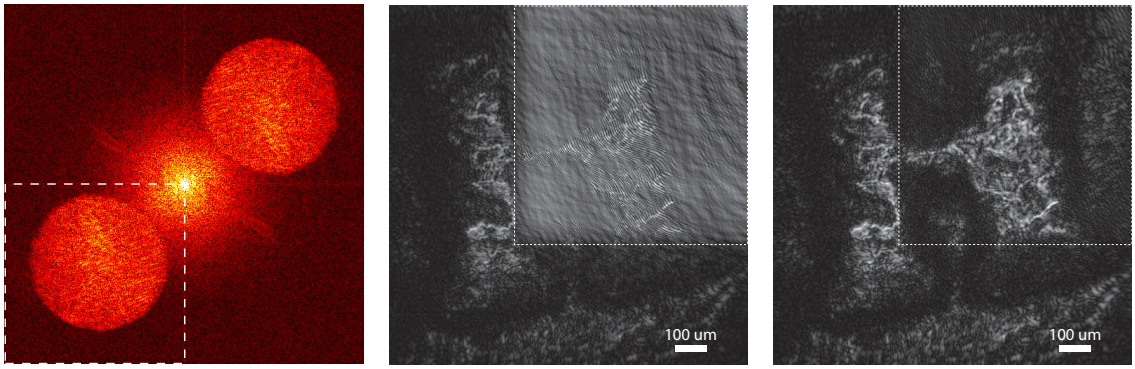

(a) (b) (c)

Figure 4: (a) Fourier tranform of the hologram made from the reflection on a coin. Amplitude of the reconstructed object field with (b) standard linear Fourier filtering and (c) the non-linear method, where the zero-order, identified by the dotted square is suppressed.

We reconstructed the hologram by filtering a quadrant of the Fourier plane (cf. dashed line in Fig. 4(a)), and employed both linear and non-linear method. The object is the letter "H" of the word "Helvetia" engraved on a Swiss coin. The zero-order can be readily identified in the amplitude reconstructed with linear filtering, as presented in Fig. 4(b), where the object auto-correlation position is emphasized with a dotted square. On the other hand, the non-linear method provides a zero-order-free amplitude, as shown in Fig. 4(c), where the auto-correlation in the top-right of the image have been suppressed, and no ghost in the reconstruction can be identified.

4.2 Resolution improvement

As stated before, suppressing the zero-order makes it possible to extend the usable bandwidth for the imaging order. We showed that in the context of off-axis DHM, enabling the use of a full quadrant of the Fourier plane leads to diffraction-limited imaging.[18] In order to demonstrate the advantage in resolution provided by suppressing the zero-order, we measured a mirror with a scratch by employing a setup using the configuration shown in Fig. 3, with a $20\times$ MO having a numerical aperture $\mathrm{NA} = 0.4$, a wavelength of $\lambda = 657$ nm, and a camera pixel size of $\Delta x = 6.45$ μm. The scratch generates strong spatial frequencies which disrupt the reconstructed phase signal.

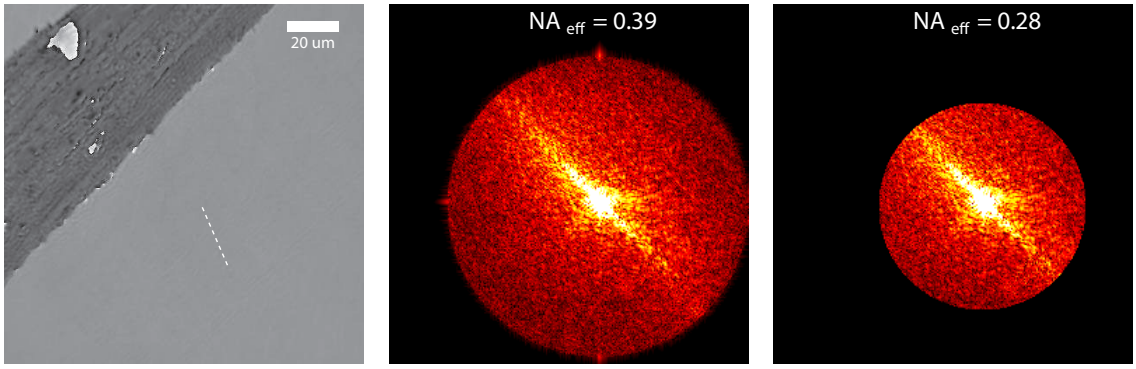

(a) (b) (c)

Figure 5: (a) Phase of the scratched mirror reconstructed with the non-linear method. (b) Quadrant of the Fourier plane containing the imaging order for the non-linear reconstruction. (c) Quadrant of the Fourier plane corresponding to the linear reconstruction, where the imaging order was filtered with a smaller bandwidth to reach the same phase standard deviation as for the non-linear method on the measured on the line shown in (a). Effective numerical apertures ($\mathrm{NA}_{\mathrm{eff}}$) corresponding to each reconstruction are shown in the spectra.

The reconstructed phase of the scratched mirror is shown in Fig. 5(a), in the case of the non-linear reconstruction method. In order to estimate the effect of the components of the zero-order which overlap with the imaging order, we filtered the spectrum after reconstruction to suppress out-of-band noise, as presented in Fig. 5(b). The imaging order has an extent of $a = 209$ pixels, so that a circular mask slightly larger was employed for filtering.

Through the diameter of the bandwidth of the imaging order, one can calculate the corresponding effective numerical aperture $\mathrm{NA}_{\mathrm{eff}}$ of the optical system as[18]

$$\mathrm{NA}_{\mathrm{eff}} = \frac{aM\lambda}{2N\Delta x} \tag{7}$$

where M is the magnification of the system, and N is the resolution of the camera in pixels. For the case of non-linear reconstruction shown in Fig. 5(b), this leads to $\mathrm{NA}_{\mathrm{eff},NL} = 0.39$, which is very close to the nominal value of the MO.

We measured the standard deviation of the phase on a line situated on the flat surface of the mirror (see dashed line in Fig. 5(a)), which gives a standard deviation for the non-linear reconstruction method of $\sigma_{NL} = 1.44°$. Measuring the standard deviation at the same location on the phase map reconstructed with the standard linear method yields $\sigma_{FT} = 2.24°$. The large difference can be explained by the remaining zero-order auto-correlation, which induces artifacts in the phase if not suppressed properly.

We then varied the diameter of the circular filter in the case of standard reconstruction in order to reach back the phase standard deviation provided by the non-linear filtering, by suppressing the zero-order through standard spatial filtering. This was reached for a diameter of 151 pixels, as shown in Fig. 5(c), leading to a standard deviation of $\sigma = 1.43°$. However, a filter of this diameter corresponds to an effective numerical aperture of $\mathrm{NA}_{\mathrm{eff},FT} = 0.28$, thus dramatically decreasing the spatial resolution of the image. This shows the ability of non-linear filtering to extend the spatial resolution of images obtained through DHM, without the cost of disrupting the phase signal with artifacts.

5. CONCLUSION

We have experimentally validated a new non-linear reconstruction technique for digital holography. This technique has been shown to be efficient for suppressing the object zero-order term. We also showed that it improves the resolution of the reconstruction, since a full quadrant of the Fourier spectrum can be used for recording, contrary to a fraction of it in the case of standard filtering. We could demonstrate this advantage experimentally in cases where the full optical resolution can be achieved while not having artifacts of the object auto-correlation. This leads to diffraction-limited imaging for off-axis digital holographic microscopy, while retaining the one-shot feature of this technique. We also showed that this method can be employed with low aperture systems for reconstructing speckle holograms.

This algorithm can be applied in standard experimental conditions. The only additional requirement is that the reference amplitude has to be stronger than that of the object, and that the imaging order has to be contained in one quadrant of the Fourier spectrum. Experiments showed that this algorithm is effective even in the case of a strong spectral overlap between the zero-order and the diffraction orders.

The proposed method is therefore particularly suitable for measurements with low magnification, where the overlap between various orders is inevitable, if one wants to keep the full resolution provided by the optical system. The image quality improvement can also be used for other recording conditions, since spectral overlap can also occur in case of high magnification measurements.

6. ACKNOWLEDGEMENTS

This research has been funded by the Swiss National Science Foundation (SNSF) grant #205320-120118. The authors would like to thank their colleagues in the MicroVision and Microdiagnostics Group, in particular E. Shaffer and J. Kühn, and at Lyncée Tec SA (www.lynceetec.com) for their cooperation and several fruitful discussions.

REFERENCES

[1] Cuche, E., Marquet, P., and Depeursinge, C., "Simultaneous amplitude-contrast and quantitative phase-contrast microscopy by numerical reconstruction of Fresnel off-axis holograms," *Appl. Opt.* **38**(34), 6994–7001 (1999).

[2] Kühn, J., Charrière, F., Colomb, T., Cuche, E., Montfort, F., Emery, Y., Marquet, P., and Depeursinge, C., "Axial sub-nanometer accuracy in digital holographic microscopy," *Meas. Sci. Technol.* **19**(7), 074007 (2008).

[3] Marquet, P., Rappaz, B., Magistretti, P. J., Cuche, E., Emery, Y., Colomb, T., and Depeursinge, C., "Digital holographic microscopy: A noninvasive contrast imaging technique allowing quantitative visualization of living cells with subwavelength axial accuracy," *Opt. Lett.* **30**(5), 468–470 (2005).

[4] Kemper, B. and von Bally, G., "Digital holographic microscopy for live cell applications and technical inspection," *Appl. Opt.* **47**(4), A52–A61 (2008).

[5] Rappaz, B., Charrière, F., Depeursinge, C., Magistretti, P. J., and Marquet, P., "Simultaneous cell morphometry and refractive index measurement with dual-wavelength digital holographic microscopy and dye–enhanced dispersion of perfusion medium," *Opt. Lett.* **33**(7), 744–746 (2008).

[6] Jacquot, P., "Speckle interferometry: A review of the principal methods in use for experimental mechanics applications," *Strain* **44**(1), 57–69 (2008).

[7] Leith, E. N. and Upatnieks, J., "Reconstructed wavefronts and communication theory," *J. Opt. Soc. Am.* **52**(10), 1123–1130 (1962).

[8] Yamaguchi, I. and Zhang, T., "Phase-shifting digital holography," *Opt. Lett.* **22**(16), 1268–1270 (1997).

[9] Takaki, Y., Kawai, H., and Ohzu, H., "Hybrid holographic microscopy free of conjugate and zero–order images," *Appl. Opt.* **38**(23), 4990–4996 (1999).

[10] Cai, L., Liu, Q., and Yang, X., "Phase-shift extraction and wave-front reconstruction in phase-shifting interferometry with arbitrary phase steps," *Opt. Lett.* **28**(19), 1808–1810 (2003).

[11] Wang, Z. and Han, B., "Advanced iterative algorithm for phase extraction of randomly phase-shifted interferograms," *Opt. Lett.* **29**(14), 1671–1673 (2004).

[12] Kreis, T. and Jüptner, W. P. O., "Suppression of the dc term in digital holography," *Opt. Eng.* **36**(8), 2357–2360 (1997).

[13] Takeda, M., Ina, H., and Kobayashi, S., "Fourier-transform method of fringe-pattern analysis for computer-based topography and interferometry," *J. Opt. Soc. Am.* **72**(1), 156–160 (1982).

[14] Chen, G.-L., Lin, C.-Y., Kuo, M.-K., and Chang, C.-C., "Numerical suppression of zero-order image in digital holography," *Opt. Express* **15**(14), 8851–8856 (2007).

[15] Weng, J., Zhong, J., and Hu, C., "Digital reconstruction based on angular spectrum diffraction with the ridge of wavelet transform in holographic phase-contrast microscopy," *Opt. Express* **16**(26), 21971–21981 (2008).

[16] Zhang, Y., Pedrini, G., Osten, W., and Tiziani, H., "Reconstruction of in-line digital holograms from two intensity measurements," *Opt. Lett.* **29**(15), 1787–1789 (2004).

[17] Seelamantula, C. S., Pavillon, N., Depeursinge, C., and Unser, M., "Zero-order-free image reconstruction in digital holographic microscopy," in [*IEEE International Symposium on Biomedical Imaging: From Nano to Macro, ISBI*], 201–204 (IEEE, 2009).

[18] Pavillon, N., Seelamantula, C., Kühn, J., Unser, M., and Depeursinge, C., "Suppression of the zero-order term in off-axis digital holography through nonlinear filtering," *Appl. Opt.* **48**(34), H186–H195 (2009).

[19] Schnars, U. and Jüptner, W. P. O., "Digital recording and numerical reconstruction of holograms," *Meas. Sci. Technol.* **13**(9), R85–R101 (2002).

[20] Colomb, T., Montfort, F., Kühn, J., Aspert, N., Cuche, E., Marian, A., Charrière, F., Bourquin, S., Marquet, P., and Depeursinge, C., "Numerical parametric lens for shifting, magnification, and complete aberration compensation in digital holographic microscopy," *J. Opt. Soc. Am. A* **23**(12), 3177–3190 (2006).

[21] Cuche, E., Marquet, P., and Depeursinge, C., "Spatial filtering for zero-order and twin-image elimination in digital off–axis holography," *Appl. Opt.* **39**(23), 4070–4075 (2000).

[22] Montfort, F., Charrière, F., Colomb, T., Cuche, E., Marquet, P., and Depeursinge, C., "Purely numerical compensation for microscope objective phase curvature in digital holographic microscopy: Influence of digital phase mask position," *J. Opt. Soc. Am. A* **23**(11), 2944–2953 (2006).

[23] Charrière, F., Colomb, T., Montfort, F., Cuche, E., Marquet, P., and Depeursinge, C., "Shot-noise influence on the reconstructed phase image signal-to-noise ratio in digital holographic microscopy," *Appl. Opt.* **45**(29), 7667–7673 (2006).